Integrated Terahertz Communication with Reflectors for 5G Small Cell Networks

Article *in* IEEE Transactions on Vehicular Technology · July 2017

DOI: 10.1109/TVT.2016.2639326

3 authors, including:

Michael Barros
Waterford Institute of Technology
39 PUBLICATIONS **61** CITATIONS
SEE PROFILE

Sasitharan Balasubramaniam
Tampere University of Technology
129 PUBLICATIONS **1,760** CITATIONS
SEE PROFILE

Integrated Terahertz Communication With Reflectors for 5G Small-Cell Networks

Michael Taynnan Barros, Robert Mullins, and Sasitharan Balasubramaniam, *Senior Member, IEEE*

***Abstract*—As the cellular networks continue to progress between generations, the expectations of 5G systems are planned toward high-capacity communication links that can provide users access to numerous types of applications (e.g., augmented reality and holographic multimedia streaming). The demand for higher bandwidth has led the research community to investigate unexplored frequency spectrums, such as the terahertz band for 5G. However, this particular spectrum is strived with numerous challenges, which includes the need for line-of-sight (LoS) links as reflections will deflect the waves as well as molecular absorption that can affect the signal strength. This is further amplified when a high quality of service has to be maintained over infrastructure that supports mobility, as users (or groups of users) migrate between locations, requiring frequent handover for roaming. In this paper, the concept of mirror-assisted wireless coverage is introduced, where smart antennas are utilized with dielectric mirrors that act as reflectors for the terahertz waves. The objective is to utilize information such as the user's location and to direct the reflective beam toward the highest concentration of users. A multiray model is presented in order to develop the propagation models for both indoor and outdoor scenarios in order to validate the proposed use of the reflectors. An office and a pedestrian-walking scenarios are used for indoor and outdoor scenarios, respectively. The results from the simulation work show an improvement with the usage of mirror-assisted wireless coverage, improving the overall capacity, the received power, the path loss, and the probability of LoS.**

***Index Terms*—5G, mirror-assisted wireless coverage, outdoor and indoor communications, smart antennas, terahertz communication.**

I. Introduction

THE evolutionary development of mobile networks has resulted in advanced technologies for both the handset and wireless access to the base stations. This development has provided users with unprecedented data rates, enabling various types of rich multimedia services to be realized (e.g., high-definition video conferencing). However, moving forward into the future, the expectations for higher data rates will increase, where this will largely be enforced from more advanced applications and services (e.g., Self-driving cars, Augmented Reality Experience, and Internet of Bio-Nano Things [1]–[4]). By 2020, the IP data handled by wireless networks are expected to exceed 500 exabytes [1], [5]. The next-generation 5G network, which is currently in the research and development stage, has laid out a set of requirements that were not fully realized by the long-term evolution technology, and these requirements include high data rate and capacity (10 Gbps), while maintaining the end-user quality of service, energy-efficient and green communication systems, and flexible management of resources. The latter requirement is particularly of great interest to the mobile network operators, where the network management of 5G networks is moving toward decoupling the data and control plane [1]. This revolutionary change will be realized through software-defined networking and network function virtualization [6].

While new forms of software deployments are being planned for 5G systems, there is also a need to discover new wireless technologies between the handset and the base stations that are able to handle very high speed transmissions. One approach that has been investigated in recent years is to push the carrier frequencies into the terahertz band in order to achieve data rate that is close to 10^{12} bps. Antennas communicating in this frequency range have been proposed for small cells with small-coverage areas. These small cells, with a range between 10 and 15 m, are able to maintain a decent level of signal quality for high end-to-end capacity in areas with high density of mobile users. Deploying these small cells that operate in parallel with the macrocells also provides an opportunity to offload traffic in order to reduce the operation costs [7].

Nevertheless, terahertz-band communication has many challenges regarding the reliability of link stability due to nonline-of-sight connections (NLoS) that exist in the environment, molecular absorptions due to the weather, and frequency response due to the Doppler effect. When signals are transmitted in the terahertz band, the data rate drops considerably for NLoS links due to reflection and/or scattering losses on rough surfaces [8], [9]. Molecular absorption also negatively impacts the communication channel, where water vapor is known to attenuate the signal. Finally, multipath propagation and the Doppler effect are known problems for outdoor scenarios, which have not been properly studied in the terahertz-band communication, and are considered highly challenging to the communication system performance [10], [11].

In order to address the issues addressed above, this paper proposes smart antennas that are designed to provide mirror-assisted coverage for 5G small cells utilizing terahertz-band

Manuscript received April 10, 2016; revised September 30, 2016; accepted November 14, 2016. Date of publication December 13, 2016; date of current version July 14, 2017. This work was facilitated by the CogNet project (671625), which is funded under the European Commission's Horizon 2020 program. The review of this paper was coordinated by Dr. S. Mumtaz.

M. Taynnan Barros and R. Mullins are with the Telecommunication Software and Systems Group, Waterford Institute of Technology, Waterford X91 P20H, Ireland (e-mail: mbarros@tssg.org; rmullins@tssg.org).

S. Balasubramaniam is with the Nano Communications Center, Department of Electronics and Communication Engineering, Tampere University of Technology, 33101 Tampere, Finland (e-mail: sasi.bala@tut.fi).

Color versions of one or more of the figures in this paper are available online at http://ieeexplore.ieee.org.

Digital Object Identifier 10.1109/TVT.2016.2639326

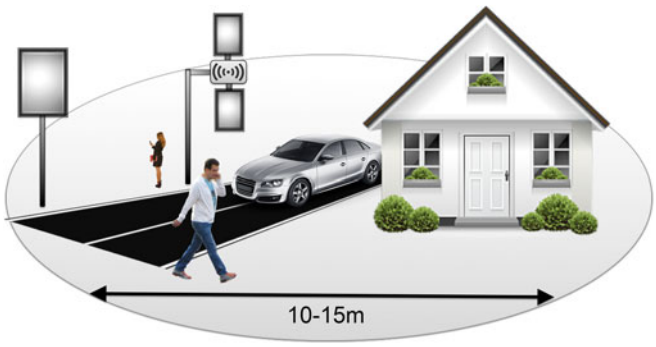

Fig. 1. Smart antennas for 5G small cells with terahertz-band communication. These antennas have a dielectric mirror coupled to each antenna and assist by reflecting signals from neighboring base stations. We term this coordination of reflectors as mirror-assisted coverage.

communication. Fig. 1 illustrates our proposed antennas for both indoor and outdoor environments. Each of the antennas contains a number of moveable dielectric mirrors that are able to adaptively reflect and direct the beams from other antennas, leading to increased signal power and gain in specific locations.

In order to provide substantial insights about the benefits of the proposed approach, a multiray channel model for wideband terahertz-band communication is presented. The model accounts for spreading, molecular absorption, reflection, and scattering losses. Two scenarios are studied in order to investigate both indoor and outdoor areas. For indoor communication, an office scenario is modeled, while for the outdoors, a walking pedestrian model is developed. For each scenario, blockage models have been obtained to study both medium and high blockage densities. For each of these scenarios, four metrics will be evaluated: path loss, received power, capacity, and probability of line of sight (LoS).

Our contribution can be summarized as follows.

1) *Mirror-assisted coverage for small cells with dielectric mirrors:* A new antenna architecture coupled to dielectric mirrors is presented for terahertz signal propagation improvements. The coverage power can be redirected and/or concentrated to specific areas through coordinated rotation of the mirrors. The benefit of this approach is to be able to beam and concentrate signal strength toward locations with high density of mobile handsets.
2) *Capacity, path loss, and received power analysis for mirror-assisted 5G small cells:* The analysis presented in this paper show a remarkable benefit for small-cell deployment that can exploit the terahertz band to improve the network capacity. This is important development toward the realization of ultradense wireless 5G networks that can provide high data rate and capacity for mobile users.
3) *The probability of LoS has been improved with mirror coordination:* Through the usage of simple mirror coordination, the probability of LoS has been improved, and the increase of the received power has been achieved with the concept of virtual LoS. The analysis presented in this paper goes through various locations within a confined space, and how the performance can be improved through coordination of mirrors.

The rest of this paper is organized as follows. Section II presents the terahertz-band communication technology and its model. Section III presents the method in using smart antennas using adaptive beamforming and reflection properties. Section IV presents the analysis for quantifying our contribution. Finally, in Section V, the conclusion of this paper is presented.

II. Terahertz-Band Communication

The most cited technology for providing high date rate satisfying 5G demands is terahertz-band communication [10]. Communicating at this band can lead to transmission up to 10^{12} bps, providing reliable 5G-based applications that require high data rate. The frequencies between 100 GHz to 10 THz can provide ultrabroadband spectrum usage, being suitable for high spectrum efficiency. While this spectrum band seems appealing, it is not fully developed for communications, and, in particular, for small cells. Currently, researchers are concentrating their efforts on accurate communication models and their validation before this technology could be deployed. The proposed models, such as in [12]–[14], present an in-depth study on the different peculiarities that are uniquely found in the terahertz band. These models, however, have scalability issues, as well as other limitations that include multiple propagation effects. Works like [15]–[17] have proposed more complete and advanced models using ray-tracing techniques for the band (0.06–1 THz). In the following, a terahertz signal propagation model is presented. It will serve as the base for validating the proposed approach of mirror-assisted antennas with reflectors for 5G terahertz-band communication in small cells.

A. Terahertz Signal Model

Aiming to present an accurate multiray propagation model for the 0.06–10-THz band communication, the ray-tracing method incorporates principles from optics. This is based on the characterization of electromagnetic waves in the studied frequency range [15] and is based on [8], [11], and [15]–[17].

The multiray model considers propagation effects, including spreading ($\Psi(f,r)$), molecular absorption ($\beta(f,r)$), reflection ($\Gamma(f,r)$), and scattering ($\zeta(f,r)$), where f is the frequency and r is the distance. In the following, each of these effects is formulated.

1) Spreading: Spreading is the effect of electromagnetic signal propagation for a LoS configuration and, in the case of the terahertz band, can be obtained in the following way [11]:

$$\Psi(f,r) = \left(\frac{c}{4\pi f r}\right)^2 \tag{1}$$

where c is the speed of light in vacuum. Particularly, the effect of spreading on the terahertz band can be quite small in terms of gain and can be an issue for long-range communication links.

2) Molecular Absorption: The molecular absorption loss impacts considerably on the terahertz signals and must be considered. This can be characterized as [11]

$$k(f) = \sum_g \frac{p}{p_0}\frac{T_0}{T}\sigma^g(f) \tag{2}$$

where p is the system pressure, p_0 is the reference pressure, T_0 is the standard temperature, T is the system temperature, and $\sigma^g(f)$ is the absorption cross section. According to [11], the major contributor to the total absorption is water vapor, and this is the only gas considered in this study.

The radiative transfer theory is used for quantification of the molecular absorption loss depending on frequency and distance. For this, the Beer–Lambert law is considered [11] and represented as

$$\beta(f,r) = e^{-\frac{1}{2}k(f)r}. \tag{3}$$

3) Reflection: The Kirchhoff theory is used for calculating the reflection loss of terahertz waves. The Fresnel reflection coefficient and the Rayleigh roughness factor are used in this analysis. The Fresnel reflection coefficient can be obtained from [8]

$$R(f) = \frac{\cos(\theta_i) - n_t\sqrt{1-(\frac{1}{n_t}\sin(\theta_i))^2}}{\cos(\theta_i) + n_t\sqrt{1-(\frac{1}{n_t}\sin(\theta_i))^2}} \tag{4}$$

where θ_i is the angle of the incident wave, and n_t is the refractive index of a medium.

The Rayleigh roughness factor can be defined as [8]

$$\rho(f) = e^{-\frac{G(f)}{2}} \tag{5}$$

with

$$G(f) = \left(\frac{4\pi\omega\cos(\theta_i)}{c}\right)^2 \tag{6}$$

where ω is the standard deviation of the surface roughness, and c is the free-space wavelength of the incident wave.

Thus, the reflection loss can be written as [15]

$$\Gamma(f,r) = \sum_n \Psi(f,r) \times \beta(f,r) \times R(f) \times \rho(f) \tag{7}$$

where n is the number of rays.

4) Scattering: Scattering affects terahertz signals based on the roughness level of the surface that it reflects itself from. This is considered critical to the communication link and must also be taken into account.

First, we consider the Beckham–Kirchhoff theory for obtaining the scattering coefficient and its approximation [15], which is represented as

$$\begin{aligned} S(f) = & -e^{\frac{-2\cos(\theta_1)}{\sqrt{n_t^2-1}}}\sqrt{\frac{1}{1+g+\frac{g^2}{2}+\frac{g^3}{6}}} \\ & \times\sqrt{p_0+\frac{\pi\cos(\theta_1)}{100}\left(ge^{v_s}+\frac{g^2}{4}e^{\frac{-v_s}{2}}\right)} \end{aligned} \tag{8}$$

where the values of p_0, g, v_s, and θ_1 can be found in [18].

Thus, the scattering loss can be obtained considering spreading, molecular absorption, the Rayleigh roughness factor, and the scattering coefficient of n rays and is represented as

$$\zeta(f,r) = \sum_n \Psi(f,r) \times \beta(f,r) \times R(f) \times S(f). \tag{9}$$

B. Path-Loss Model

A path-loss model can be obtained by adding the attenuation loss of each signal propagation effect [spreading (Ψ), molecular absorption (β), reflection (Γ), and scattering (ζ)] in decibels, and this is represented as

$$\begin{aligned} \alpha(f,r) = & \ 10\times\log_{10}(\Psi(f,r)) + 10\times\log_{10}(\beta(f,r)) \\ & +10\times\log_{10}(\Gamma(f,r)) + 10\times\log_{10}(\zeta(f,r)). \end{aligned} \tag{10}$$

C. Received Power Model

Link budget analysis is used to model the received power in the terahertz-band communication for 5G systems. This technique is in accordance with previous studies for millimeter-wave communication and also terahertz communication [9]. The following formula is used:

$$R_{px} = P_{tx} + G_{tx} + G_{rx} - \alpha(f,r) - \gamma \tag{11}$$

where R_{px} is the received power, P_{tx} is the transmission power, G_{tx} is the antenna gain in the transmitter, G_{rx} is the antenna gain in the receiver, and γ is the loss resulting from shadowing.

For an in-depth analysis for quantifying the contribution of the paper, the received power model is separated for both indoor and outdoor scenarios. They are presented in the following.

1) Indoors: The indoor scenario is characterized by an area of 5 × 5 m, resulting in a realistic office setting under room temperature. Parameter values from [9] were used: $P_{tx} = 1$ dBm with 7.4-dB conversion loss; G_{tx} and G_{rx} are equal to 30 dBi. However, the receiver has a conversion gain of 8 dB with a noise figure of 7.5 dB and $\gamma = -74$ dBm. This results in

$$R_{pi} = 127.7 - \alpha(f,r). \tag{12}$$

2) Outdoors: For the outdoor scenario, an area of 20 × 20 m is used to simulate a moving pedestrian. Signal reflection and scattering is found in the environment, as they are reflected from building walls as well as other objects in the environments (e.g., trees and benches) (in this scenario, we consider a pedestrian walking along a path in the city center that is lined with buildings). Parameters values from [23]–[26] were used: $P_{tx} = 2$ dBm; G_{tx} and G_{rx} are equal to 21 dBi. The receiver has a conversion gain of 8 dB with a noise figure of 7.5 dB and $\gamma = -50$ dBm. This results in

$$R_{pi} = 141.7 - \alpha(f,r). \tag{13}$$

D. Blockage Model

Using the simple regression model analysis obtained from [19]–[22], the blockage analysis is presented in the following through the calculation of the probability of LoS. The indoor scenario is modeled according to an office-like environment, which includes an open-plan office with cubical area, a closed-plan office with corridor and meeting room, and also a hybrid-plan office with both open and closed areas. On the other hand, the outdoor scenario is accountable for buildings in an urban scenario, which is based on the 3GPP 3-D model. All models, including both medium and high blockage densities, are found in Table I.

TABLE I
PROBABILITY OF LOS MODELS OBTAINED FROM [19]–[22]

	Medium Blockage Density	High Blockage Density
Indoor	$\text{plos}(d) = \begin{cases} 1, & \text{if } d <= 1.2 \\ \exp -\frac{d-1.2}{4.7}, & \text{if } 1.2 < d \leq 6.5 \\ \exp -\frac{d-6.5}{32.6} * 0.32, & \text{if } d > 6.5 \end{cases}$	$\text{plos}(d) = \begin{cases} 1, & \text{if } d <= 1.2 \\ \exp -\frac{d-1.2}{2.35}, & \text{if } 1.2 < d \leq 6.5 \\ \exp -\frac{d-6.5}{16.3} * 0.32, & \text{if } d > 6.5 \end{cases}$
Outdoor	$\text{plos}(d) = \begin{cases} 1, & \text{if } d <= 1.2 \\ \exp -\frac{d-1.2}{40}, & \text{if } 1.2 < d \leq 6.5 \\ \exp -\frac{d-6.5}{82.5}, & \text{if } d > 6.5 \end{cases}$	$\text{plos}(d) = \begin{cases} 1, & \text{if } d <= 1.2 \\ \exp -\frac{d-1.2}{80}, & \text{if } 1.2 < d \leq 6.5 \\ \exp -\frac{d-6.5}{165}, & \text{if } d > 6.5 \end{cases}$

E. Capacity Model

In order to evaluate the capacity based on the presented propagation model, we use a wideband window model dividing the terahertz-band into subband channels. This is necessary due to the inherent frequency-selective characteristic of the terahertz channel. A number of i subband channels are selected with a Δf width each. The resulting channel capacity is represented as

$$C(d) = \sum_i \Delta f \log_2 \left[1 + \frac{\alpha(f,r)^{-1} S_i}{N_0}\right] \tag{14}$$

where S_i is the transmitting power p.s.d., and N_0 is the noise p.s.d. and is considered flat for all the subbands [27]. More investigation into the noise in the terahertz band is still required [10].

III. SMART ANTENNAS FOR 5G TERAHERTZ-BAND COMMUNICATION

Based on the numerous issues that are imposed from communicating in the terahertz band, the usage of smart antennas and mirrors for enabling mirror-assisted wireless coverage is proposed in this paper. Mirror-assisted wireless coverage can reflect rays that beam to a concentrated area, where the total signal reception will have higher strength. The mirror-assisted wireless coverage for terahertz-band communication can be beneficial for the three issues discussed in Section I (i.e., NLoS connections, molecular absorption, and node mobility). Due to the refractive index of mirrors, NLoS signals that are reflected by them are not affected by rough surfaces. Wireless signal coverage can also be redirected adaptively to areas with lower molecular absorption loss. Finally, mirror-assisted wireless coverage can be beneficial for locations with different densities of end-user handsets and adaptively changes the critical coverage area as the nodes migrate. In the following, a deeper investigation will be explored for the smart antenna structure, terahertz signal reflection, antenna beam adaptation, and, finally, mirror-assisted wireless coverage.

A. Smart Antenna Structure

The full structure of the proposed smart antennas is shown in Fig. 2. The dielectric mirrors are coupled to the antenna structure in order to provide reflections of terahertz signals with minimum attenuation possible. Although they are attached to the antenna itself, it is used to reflect the signals from the neighboring base stations, rather than its own. It is envisioned that the dielectric mirrors have motors attached to their interior surface, which will allow them to rotate and adaptively change their

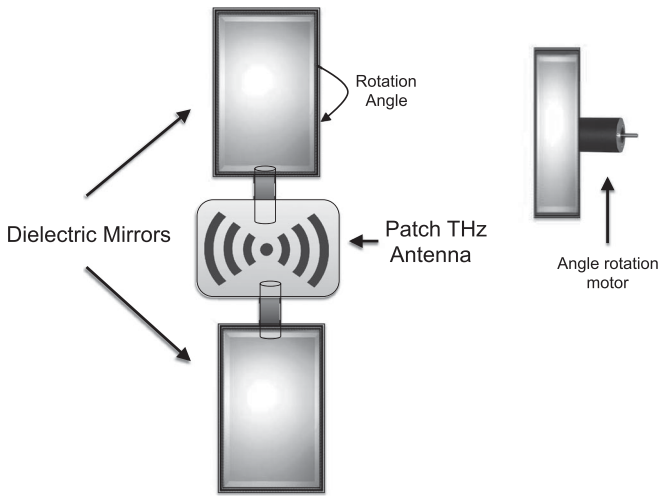

Fig. 2. Structure of the smart antennas for terahertz-band communication in 5G small cells. Dielectric mirrors are coupled to the antenna structure. These mirrors allow reflection of terahertz waves. Also, they are able to change their angle to adaptively change the antennas' focus.

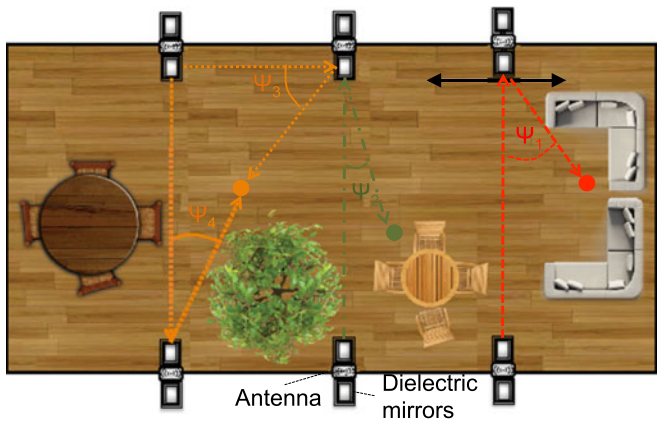

Fig. 3. Demonstration of mirror angle adaptation allowing redirection of rays to a particular spot, enabling a critical coverage area.

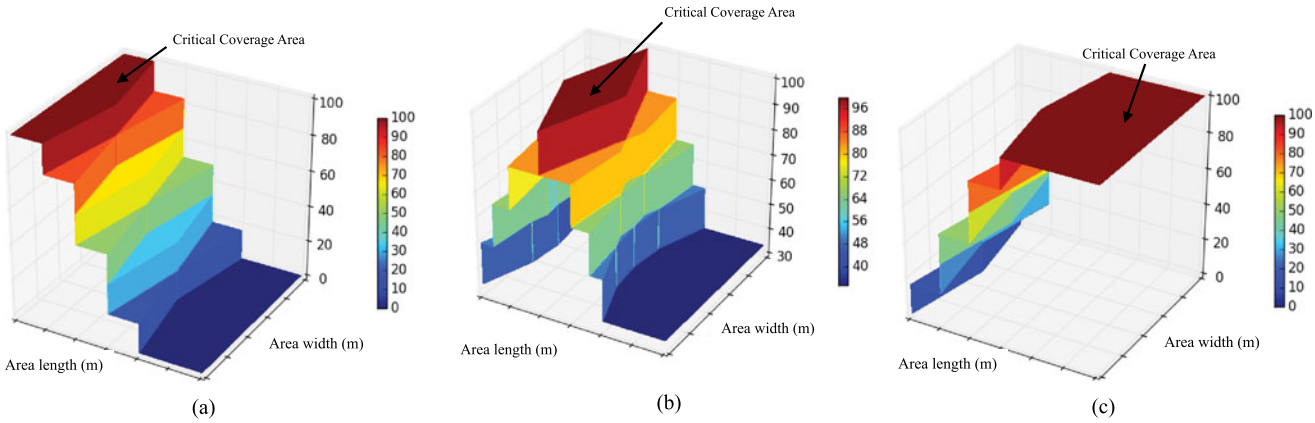

Fig. 4. Virtual LoS following left, center, and right orientation according to the intended positioning of the critical coverage areas. (a) Percentage of received rays for left orientation. (b) Percentage of received rays for center orientation. (c) Percentage of received rays for right orientation.

configuration. This, in turn, will satisfy the requirements of having a decoupled network control plane, as part of the vision of 5G. In order to satisfy this, knowledge with regard to the transmitter and receiver positions is required, and this information can be provided from the control plane. In the case of using multiple mirrors, these can cooperatively change the focus to a specific location, named critical coverage area. Fig. 3 illustrates the coordination of mirror angles directing rays to a critical coverage area. In that location, the signal strength will be aggregated to give priority to specific locations of the environment that may consist of high density of nodes.

B. Reflecting Terahertz Signals

The mirrors are composed of multiple thin layers of dielectric material with the possibility of optical coating that enables the selection of specific wavelengths that can be reflected. These mirrors are cheap, and reflection of terahertz-band waves is completely viable [28]. Piesiewicz *et al.* [29] have proposed a scenario using dielectric mirrors, in which the interior of a room would be totally covered to allow reflection. Even though the benefits of such an approach are remarkable, the impracticability of requiring walls covered with dielectric mirrors reduces the attractiveness of the proposed technology and will lead to high costs.

For reflecting NLoS signals, mirrors should have a broad range of incident angles. One approach to satisfying this requirement is the usage of omnidirectional mirrors [30]. However, for perfectly reflecting signals between a transmitter and a receiver, the beams of the antennas should be synchronized, in which beams should be pointing to each other or the mirrors. In the case of an obstacle, the reflection through a mirror creates a virtual LoS. For that, the following is required.

1) The mirrors need to adaptively change to compensate the rays' incident angle.
2) The mirrors should know the transmitter and receiver location and adaptively change their angles to provide a virtual visibility between them.
3) Antenna beams of both the transmitter and the receiver should be pointing toward the mirror.

These challenges require proper knowledge of the network infrastructure and the current status of the users within the area.

C. Antenna Beam Adaptation

We assume a linear smart antenna array with N nodes and the total gain of GT_x for the transmitter and GR_x for the receiver [31]. We also assume perfect conditions for beamforming, beamsteering, and beamwidth for the usage of the virtual LoS concept, which can be further explained in the following.

1) *Beamforming*: Adaptive antenna beamforming is an existing technique for providing directional signals without moving the transmitters and receivers. In the context of smart antennas with dielectric mirrors, we need to create a virtual LoS, as described earlier. While reflecting terahertz rays, the antenna beamforming will point the direction toward dielectric mirrors, which will reflect the signals with minimum attenuation.
2) *Beamsteering*: The smart antennas have to perform beamsteering for synchronization of the main lobe with the mirror, which is fundamental for realizing the virtual LoS. Let Ψ_i be the angle between the upper (bottom) side of the area and the smart antenna boresight (see Fig. 3). We assume that Ψ_i takes values in $G = [-\frac{\pi}{2}, \frac{\pi}{2}]$. As such, the main lobe of each smart antenna is always directed toward the area of transmission.
3) *Beamwidth*: Beamwidth is another smart antenna characteristic that has fundamental importance on the virtual LoS. The patch THz antenna can control the beamwidth adaptively [32], allowing the synchronization of the T_x antenna 3-dB zone with the mirror.

D. Mirror-Assisted Wireless Coverage

Combining the adaptive antenna beamforming with dielectric mirrors can achieve mirror-assisted wireless coverage. The adaptive in this case is when the beams are directed toward the highest number of users by only turning the angles of the dielectric mirrors. In this subsection, graphical visualization of the virtual LoS is illustrated in Fig 4. A fixed area is assumed with six mirrors placed on the two opposite walls. Three situations

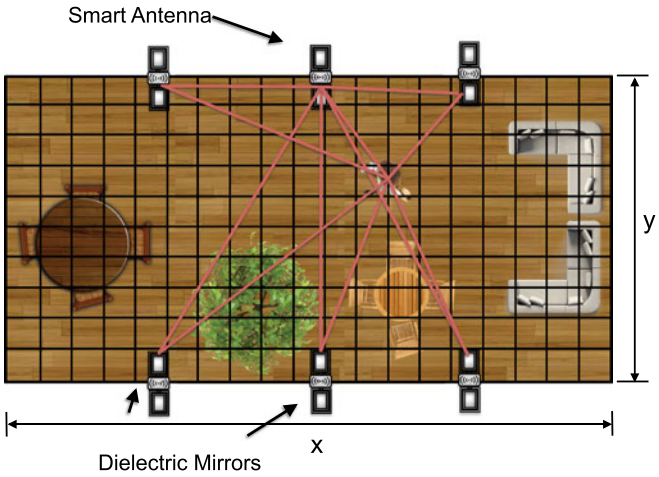

Fig. 5. Scenario used for distance analysis. The antenna is placed in the central-top position of the area. This scenario is used for both the adaptive and mirror-assisted coverage.

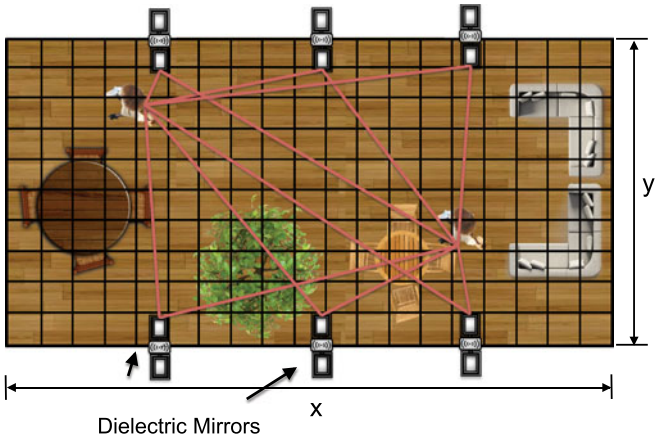

Fig. 6. Scenario used for frequency analysis. The transmitter (T_x) is placed in the center of the area and the receiver (R_x) a few meters away.

are shown, where the critical coverage area is intended to be on the left, in the center, and on the right side of the area. A uniform distribution is assumed for the reflected rays from all the mirrors. The beamforming of the antenna is very important for an optimal signal reception; however, this characteristic is neglected in this analysis, since the intention is to only show the percentage of the reflected rays. The aim here is to show that the maximum percentage of the reflected rays for the virtual LoS is obtained inside the critical coverage area.

IV. Analysis

In order to evaluate the proposed smart antenna approach (mirror-assisted coverage), and to theoretically compare to the conventional terahertz-band performance (static coverage), an extensive analysis is developed based on the ray-tracing algorithm. The analysis considers the path loss, the received power, the capacity, and the probability of LoS for both indoor and outdoor communication scenarios with medium and high blockage densities. In the following subsection, a description of the

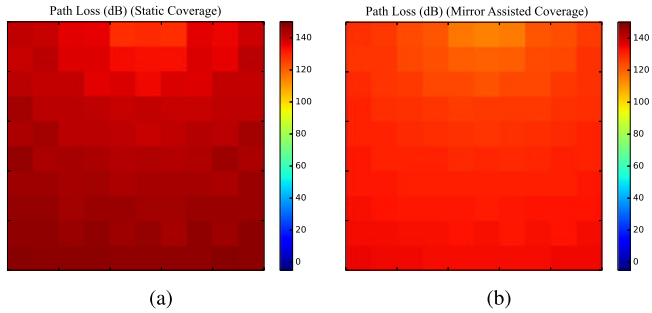

Fig. 7. Heatmap of path loss of a 10 × 10 m area with 10 × 10 tiles. The frequency used is 0.3 THz. (a) Static coverage and (b) mirror-assisted coverage.

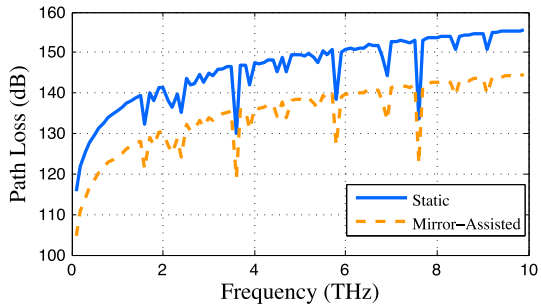

Fig. 8. Path loss as a function of frequency (THz) for a 10 × 10 m area with 10 × 10 tiles. The distance between T_x and R_x is 1 m.

ray-tracing algorithm is first described followed by the results of the analysis.

A. Ray-Tracing Simulation

A ray-tracing algorithm was developed for the insertion of the propagation loss model resulting from spreading, molecular absorption, scattering, and reflection effects in the terahertz-band communication. The developed technique was based on [9], [15], and [26]. For an area with dimensions of x and y meters containing $n \times m$ number of tiles, the ray-tracing algorithm proceeds with the following four steps:

1) reflection/scattering points are determined, as well as mirror placements;
2) placement of the transmitter (T_x);
3) computation of the incident angles based on the defined rays;
4) computation of the capacity, the received power, the path loss, and the probability of LoS according to the modeling presented in Section II for each tile of the area.

The dielectric mirrors are modeled based on their refractive properties. According to [29], the refractive index (n_t) is 3.418. These mirrors consist of four 63-μm-thick layers of high-resistant silicon. This property can easily be added to the Fresnel reflection coefficient in (4). Based on this, the rays that hit the mirrors are attenuated based on their refractive index.

Two approaches are compared: static and mirror-assisted coverage. In the first, the antennas are used with no antenna beam adaptation or mirrors. In the latter case, the antennas incorporate the beam adaptation and are able to point to the receiver direction, utilizing the dielectric mirrors for signal reflections.

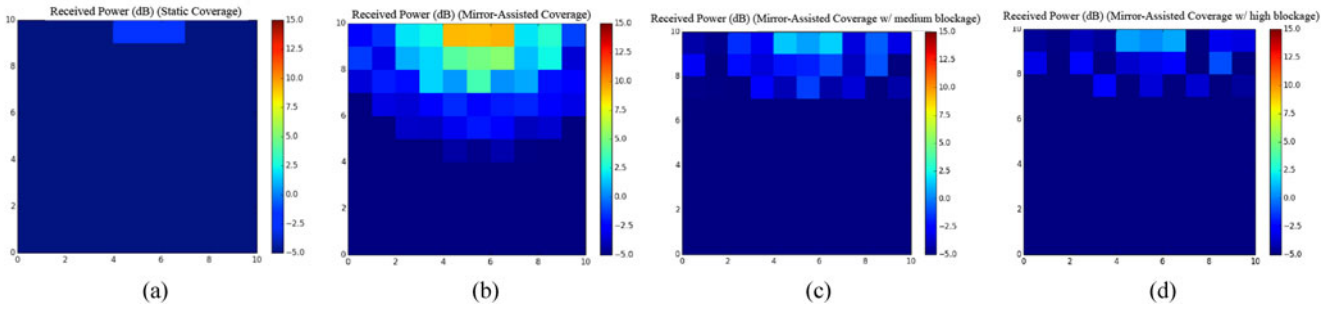

Fig. 9. Heatmap of the received power for an indoor communication scenario of a 5 × 5 m area with 5 × 5 tiles, and the frequency used is 0.3 THz. Four scenarios are considered: (a) static coverage, (b) mirror-assisted coverage with no blockage, (c) mirror-assisted with medium blockage, and (d) mirror-assisted with high blockage.

For the distance analysis, the antenna is placed on the central-top position of the area, as illustrated in Fig. 5. In the case of the frequency analysis, the transmitter (T_x) is placed in the center of the area and the receiver (R_x) a few meters away, as illustrated in Fig. 6. For the frequency analysis, the band range considered is divided into subbands.

B. Path Loss

The path loss, represented in (10), has a frequency–distance dependence, which is explored in this subsection. The distance analysis of the path loss is illustrated through heatmaps in Fig. 7. For each tile within the 10 × 10 m space, the mirror-assisted coverage will direct the mirrors to beam the rays toward that specific tile. Therefore, each tile has lower path loss intensity for the mirror-assisted coverage compared with the static. This is due to the rays that were previously attenuated based on the reflection and scattering of rough surfaces in the static coverage case are redirected through the dielectric mirrors compensating for lower total path loss in each tile.

This is also the same for frequency variation illustrated in Fig 8. The path loss increases with the frequency, and this is due to the molecular absorption loss. The distribution of water vapor over frequency and distance is given by (3). However, once again, the mirror-assisted case improves the path loss as the frequency varies to the higher end of the terahertz spectrum.

C. Indoor Environment

An office scenario is explored for the indoor environment, where the room area is 5 × 5 m with standard temperature and pressure to maintain the proper level of water vapor. In this analysis, we are keen to investigate the received power using the model in (12) and, in particular, the performance when the environment contains different quantities of objectives and blockages. For the case of objects placed in the room, the medium and high blockage densities are represented in Table I.

Fig. 9 presents the results of the total power on each tile in the room and is represented through heatmaps. The quantity of intensity on each tile shows that the received power has been increased when the mirrors are tilted at the right angle to direct the beams to right location. Fig. 9 also illustrates the effects of medium and high blockage within the room and how these affect the total power in each tile. As illustrated in Fig. 9(c), the medium blockage is still able to recover a certain amount of power with the reflections from the mirrors, and this performance is slightly decreased in the case of high blockage in Fig. 9(d).

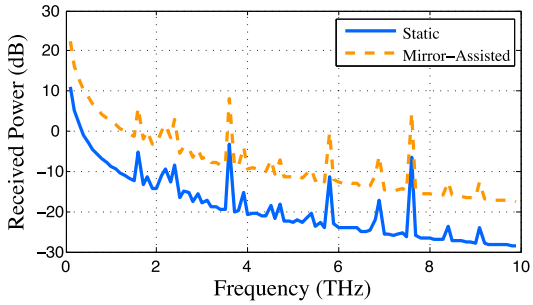

Fig. 10. Indoor communication received power as a function of frequency (THz) for a 5 × 5 m area with 5 × 5 tiles. The distance between the transmitter and the receiver is 1 m.

Fig. 10 presents the received power for both static and mirror-assisted coverage techniques as the frequencies vary. As expected, the results show that the coordinated dielectric mirrors improve the received power even when the higher frequencies suffer from power degradation due to molecular absorption.

D. Outdoor Environment

A mobile pedestrian scenario is explored for the outdoor environment analysis, where the area considered is 20 × 20 m space that contains a single road with a pedestrian walkway on the side. The side of the road also contains buildings on either sides where the antenna and the mirrors are placed. Medium and high blockage densities are characterized by the number per area of buildings and/or vehicles that can completely block the LoS connection. Similar to the indoor environment analysis, the analysis of the received power for the outdoor environment is represented by (13).

Fig. 11 presents the heatmap analysis of the received power comparison between static coverage and mirror-assisted coverage with no blockage, medium blockage, and high blockage. Similar to the indoor case, the mirror-assisted coverage leads to higher power for each tile, and we can see that the signals are reflected through neighboring mirrors to improve the performance for medium and high blockages. The blockage analysis is crucial for the outdoor case due to large objects (trees and lamp

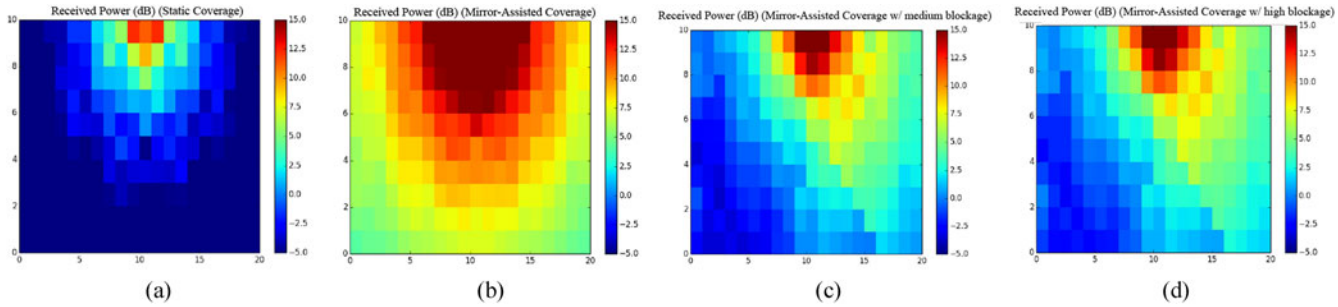

Fig. 11. Heatmap of the received power for an outdoor communication scenario of a 20 × 20 m area with 10 × 10 tiles, where the transmitter frequency used is 0.3 THz. Four scenarios are considered: (a) static coverage, (b) mirror-assisted coverage with no blockage, (c) mirror-assisted coverage with medium blockage, and (d) mirror-assisted coverage with high blockage.

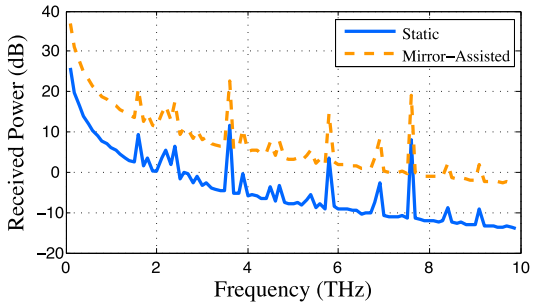

Fig. 12. Outdoor communication received power as a function of frequency (THz) for a 20 × 20 m area with 10 × 10 tiles. The distance between the transmitter and the receiver is 2 m.

posts) and mobile objects (vehicles) within the environment that can lead to high amount of scattering when the signals are reflected. At the same time, the outdoor case also has variations in the amount of molecular vapor that affects the signal absorption with 10% of water vapor. Therefore, the dynamic movements of the mirrors are very important to enable the signals to bounce around the high blockage areas to reach the receivers.

Fig. 12 shows the received power performance with respect to the variations in frequencies. As expected, the mirror-assisted coverage once again will reflect the signals around the blockages even the higher frequencies are more sensitive.

E. Impact on the Probability of LoS

This section presents the model for the probability of LoS based on the reflection from the mirrors. Consider an area of X and Y dimensions with n mirrors spread across the borders of the space. A uniform distribution is used to position the mirrors in the space with mirror $m = [m_x, m_y], m_x \in (1, X-1)$ and $m_y \in (0, Y)$. Now, consider

$$M = \begin{bmatrix} m^{(1)} \\ m^{(2)} \\ \vdots \\ m^{(n)} \end{bmatrix} \tag{15}$$

as the matrix of mirrors and their positioning.

The probability of a single-link LoS for a transmitter ($T_x = [T_{xx}, T_{xy}]$), a receiver ($T_x = [T_{xx}, T_{xy}]$), and a single mirror ($m^{(i)}$) is represented as

$$P_{\text{los}M}(Tx, Rx, i) = \int_{m_x}^{m'_x} P_{\text{los}}(d(T_x, m^{(i)}))dx \times \int_{m_x}^{m'_x} P_{\text{los}}(d(m^{(i)}, R_x))dx \tag{16}$$

where m'_x is the final position of the mirrors with length $L = m'_x - m_x$.

Therefore, the total probability of LoS (TP_{los}) is achieved by

$$\text{TP}_{\text{los}} = (P_{\text{los}}(Tx, Rx) + \sum_{i=1}^{n} P_{\text{los}M}(Tx, Rx, i)) \times \frac{1}{n+1}. \tag{17}$$

Fig. 13 presents the impact of the reflected signals from the mirrors on the probability of LoS for both the indoor and outdoor environments. For each environment, both medium and high blockage densities are considered. The probability is analyzed as a function of both the communication distance (ranging from 0 to 9 m) and the mirror size (ranging from 0 to 1 m for indoor and from 0 to 5 m for outdoor environment). Square-shaped mirrors are also considered. The results show that the probability of LoS slightly varies as the communication distance increases, but increases significantly as the mirror size changes for the outdoor environment compared with the indoor environment. The size of mirrors is selected to be proportional to the size of the room as well as the power of emitted signals. The mirror size does not have a major impact for the indoor case, but slightly increases as the size gets larger. However, in the outdoor case, the power of the signal also meant more reflections in the environment making the mirrors leading to higher probability of LoS. The size of the mirrors saturates at a particular point, making the probability of LoS saturate after the length size of 2 m. Also, for both indoor and outdoor, the variations of the communication distances do not have a dramatic effect on the probability of LoS.

F. Mirror Coordination and Blockage Analysis

Although in the power analysis for both indoor and outdoor increase for each tile within the environmental space, this assumes that each of the mirrors are coordinated to project the

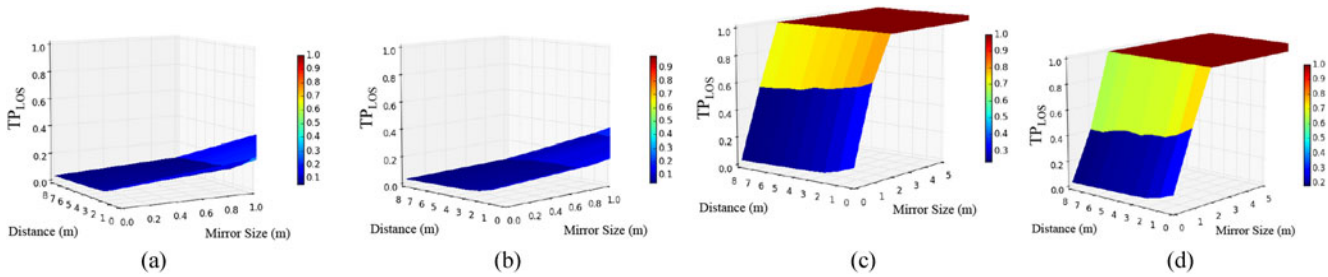

Fig. 13. Impact of the terahertz signal reflection using mirrors on the probability of LoS for both indoors and outdoors versus both medium and high blockage densities. The probability is analyzed as a function of both the communication distance (ranging from 0 to 9 m) and the mirror size (ranging from 0 to 1 m in indoors and from 0 to 5 m in outdoors.) (a) Indoor medium blockage density. (b) Indoor high blockage density. (c) Outdoor medium blockage density. (d) Outdoor high blockage density.

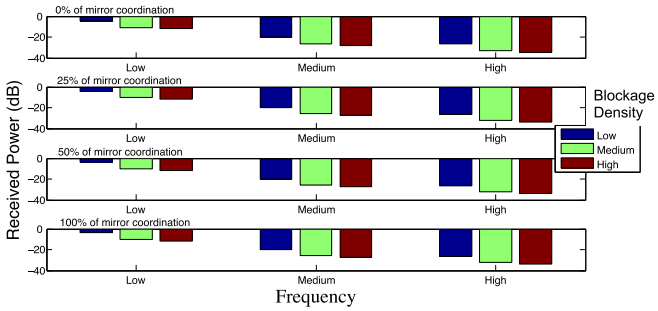

Fig. 14. Relationship of mirror coordination (0%, 25%, 50%, 100%), frequency [low (0.3 THz), medium (2 THz), and high (4 THz)], and blockage density (low, medium, and high) on the received power in indoor environments.

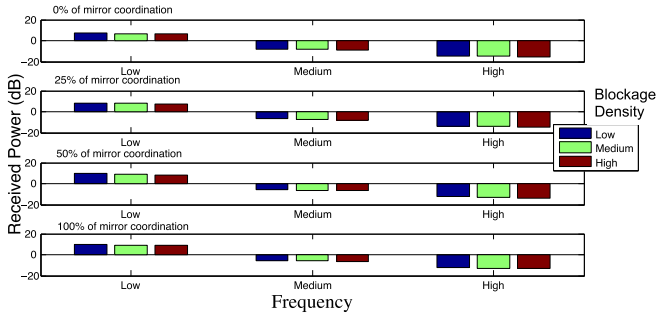

Fig. 15. Relationship of mirror coordination (0%, 25%, 50%, 100%), frequency [low (0.3 THz), medium (2 THz), and high (4 THz)], and blockage density (low, medium, and high) on the received power in outdoor environments.

reflected signal towards specific locations. Therefore, an important requirement is to ensure that coordination of the mirrors is performed, which is an analysis conducted in this section. In Fig. 14, the relationship of mirror coordination (0%, 25%, 50%, 100%), low (0.3 THz), medium (2 THz), and high (4 THz) frequencies and varying blockage densities (low, medium, and high) on the received power for indoor environments is presented. The coordination refers to the ratio of mirrors that are synchronized and reflect the signal to the right tile within the space. For each of the frequency value, the coordination of mirrors does not significantly improve the performance. Thus, the increase in blockage densities does affect the performance even when there is increased mirror coordination. Finally, the coordination does not affect the frequency of the signals dramatically.

Fig. 15 presents the same analysis for the case of the outdoor environment. Compared with the indoor case, the outdoor environment has a more positive effect from the mirror coordination, even when the quantity of blockage increases. The positive impact is due to the longer communication distances where the mirrors have an impact on longer range of directional angles and, therefore, can achieve better coverage areas. This helps to improve the received power performance in specific tile spots in the area.

G. Capacity Analysis

The capacity of a terahertz communication, represented by (14), has a frequency–distance dependence relationship, which will be explored in this section. Both the power and noise p.s.d. are kept constant for our analysis, based on [11], [15], and [27].

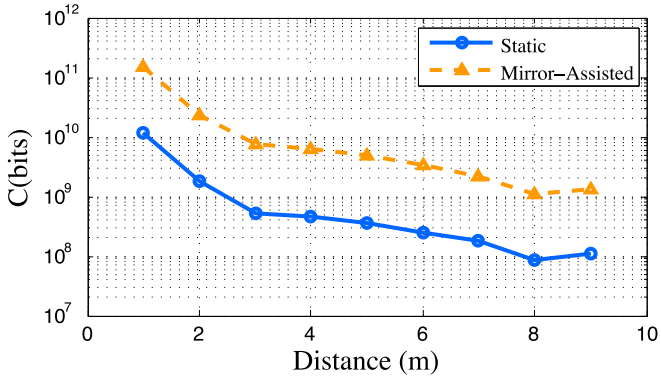

Fig. 16. Capacity as a function of distance for a 10 × 10 m area with 10 × 10 tiles. The frequency used is 0.3 THz and Δ_f is 10 THz.

Capacity is improved using adaptive coverage over the distance increase. Terahertz-band communication performance is favorable for short-range distances and decreases exponentially as the distance increases. However, as illustrated in Fig. 16, the mirror-assisted coverage can improve the overall capacity by nearly ten times compared with the static case.

Similar to the distance variation, the variations in the frequency also affect the capacity performance (Fig. 17). The higher the frequency, the more unstable it is and gets affected

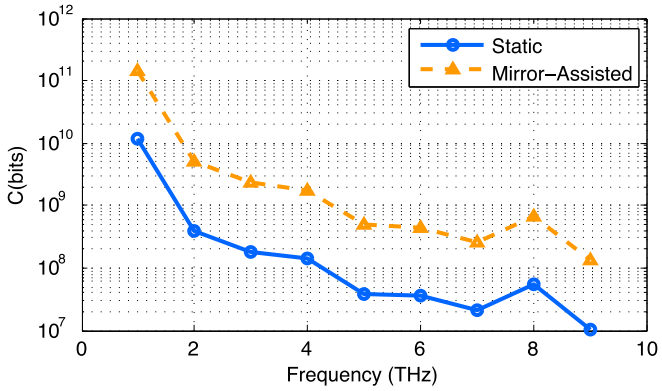

Fig. 17. Capacity as a function of frequency (THz) for a 5 × 5 m area with 5 × 5 tiles. The distance between the transmitter and the receiver is 1 m, and Δ_f is 1 THz. Both static and adaptive coverage are studied.

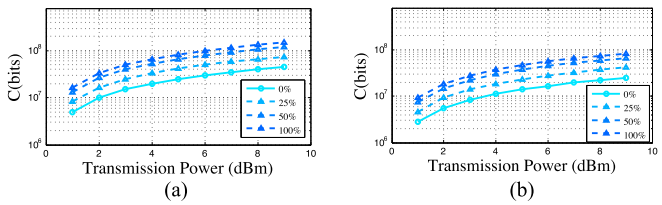

Fig. 18. Relationship between the transmission power, medium and high blockages, coordination of mirrors, and capacity for indoor environments. (a) Medium blockage density. (b) High blockage density.

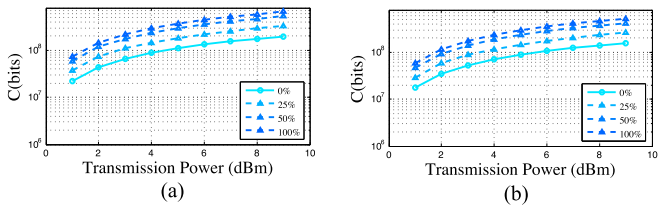

Fig. 19. Relationship between the transmission power, medium and high blockages, coordination of mirrors, and capacity for outdoor environments. (a) Medium blockage density. (b) High blockage density.

by the quantity of molecular vapor within the air, leading to reduced capacity. However, we can observe that, at around 8 THz, there is a small increase in the capacity, and this is due to the frequency-selective characteristics of high terahertz frequency that are affected by molecular absorption. At this point, the mirror-assisted coverage will improve the performance by reflecting the signals round the regions with high quantity of water vapor.

Figs. 18 and 19 present the capacity results based on the relationship between the transmission power, medium and high blockages, and coordination of mirrors for indoor and outdoor environments, respectively. For all the results, the transmission power has a linear dependence with the capacity. As observed in the results, increasing the transmission power is highly beneficial to the capacity, although this comes at a cost of higher power. Due to the density of blockage, the capacity decreases for higher blockage density, but this performance increases due to the mirrors. The outdoor environment results in higher capacity due to the antenna gain for both the receiver and the transmitter. The presented results can be correlated with the analysis presented in Figs. 14 and 15.

V. Conclusion

The growth of IP data traffic that needs to be handled by future wireless networks (5G) is motivating the need for radical changes toward network flexibility. Future 5G requires high-data-rate transmission, and few technologies are currently being developed for that. Terahertz-band communication is the leading alternative to providing 5G with data rate up to 10^{12}. However, many challenges still inhibit terahertz-band communication, including NLoS links, molecular absorption loss, and mobility. Based on this, the usage of smart antennas is suggested for terahertz-band communication. These antennas are capable of reflecting wireless signals, creating a virtual LoS. Such a technique mitigates losses from rough surfaces. However, beam synchronization between the transmitter and the receiver is required, and therefore, smart antennas must be used. Based on this, the concept of mirror-assisted wireless coverage was introduced.

To validate and provide insights into the mirror-assisted wireless coverage performance, a multiray propagation model was presented, accounting for spreading, molecular absorption, reflection, and scattering losses. Indoor and outdoor communications were studied using the ray-tracing simulation. Also, medium and high blockage densities were analyzed with a blockage analysis for both indoors and outdoors. The system showed great improvement in the light of the capacity, the received power, the path loss, and the probability of LoS. The presented approach has a tremendous potential to realizing 5G small-cell networks using terahertz-band communication.

References

[1] J. G. Andrews *et al.*, "What will 5g be?" *IEEE J. Sel. Areas Commun.*, vol. 32, no. 6, pp. 1065–1082, Jun. 2014.
[2] E. Larsson, O. Edfors, F. Tufvesson, and T. Marzetta, "Massive MIMO for next generation wireless systems," *IEEE Commun. Mag.*, vol. 52, no. 2, pp. 186–195, Feb. 2014.
[3] Y. Niu, Y. Li, D. Jin, L. Su, and A. V. Vasilakos, "A survey of millimeter wave communications (mmwave) for 5G: Opportunities and challenges," *Wireless Netw.*, vol. 21, no. 8, pp. 2657–2676, 2015.
[4] I. F. Akyildiz, M. Pierobon, S. Balasubramaniam, and Y. Koucheryavy, "The internet of bio-nano things," *IEEE Commun. Mag.*, vol. 53, no. 3, pp. 32–40, Mar. 2015.
[5] J. Andrews, "The seven ways HetNets are a paradigm shift," *IEEE Commun. Mag.*, vol. 51, no. 3, pp. 136–144, Mar. 2013.
[6] I. F. Akyildiz, S.-C. Lin, and P. Wang, "Wireless software-defined networks (W-SDNs) and network function virtualization (NFV) for 5G cellular systems: An overview and qualitative evaluation," *Comput. Netw.*, vol. 93, Part 1, pp. 66–79, 2015.
[7] I. F. Akyildiz, E. Chavarria-Reyes, D. M. Gutierrez-Estevez, R. Balakrishnan, and J. R. Krier, "Enabling next generation small cells through femtorelays," *Phys. Commun.*, vol. 9, pp. 1–15, 2013.
[8] C. Jansen, R. Piesiewicz, D. Mittleman, T. Kurner, and M. Koch, "The impact of reflections from stratified building materials on the wave propagation in future indoor terahertz communication systems," *IEEE Trans. Antennas Propag.*, vol. 56, no. 5, pp. 1413–1419, May 2008.
[9] C. Jansen *et al.*, "Diffuse scattering from rough surfaces in THz communication channels," *IEEE Trans. THz Sci. Technol.*, vol. 1, no. 2, pp. 462–472, Nov. 2011.
[10] I. F. Akyildiz, J. M. Jornet, and C. Han, "TeraNets: Ultra-broadband communication networks in the terahertz band," *IEEE Wireless Commun.*, vol. 21, no. 4, pp. 130–135, Aug. 2014.

[11] J. M. Jornet and I. F. Akyildiz, "Channel modeling and capacity analysis for electromagnetic wireless nanonetworks in the terahertz band," *IEEE Trans. Wireless Commun.*, vol. 10, no. 10, pp. 3211–3221, Oct. 2011.
[12] S. Priebe, M. Kannicht, M. Jacob, and T. Krner, "Ultra broadband indoor channel measurements and calibrated ray tracing propagation modeling at THz frequencies," *J. Commun. Netw.*, vol. 15, no. 6, pp. 547–558, 2013.
[13] H. J. Song *et al.*, "Terahertz wireless communication link at 300 GHz," in *Proc. IEEE Top. Meeting Microw. Photon.*, 2010, pp. 42–45.
[14] T. Krner and S. Priebe, "Towards THz communications—Status in research, standardization and regulation," *J. Infrared, Millimeter THz Waves*, vol. 35, no. 1, pp. 547–558, 2014.
[15] C. Han, A. O. Bicen, and I. F. Akyildiz, "Multi-ray channel modeling and wideband characterization for wireless communications in the terahertz band," *IEEE Trans. Wireless Commun.*, vol. 14, no. 5, pp. 2402–2412, May 2015.
[16] C. Han, A. O. Bicen, and I. F. Akyildiz, "Multi-wideband waveform design for distance-adaptive wireless communications in the terahertz band," *IEEE Trans. Signal Process.*, vol. 64, no. 4, pp. 910–922, Feb. 2016.
[17] S. Priebe and T. Kurner, "Stochastic modeling of THz indoor radio channels," *IEEE Trans. Wireless Commun.*, vol. 12, no. 9, pp. 4445–4455, Sep. 2013.
[18] J. Harvey, A. Krywonos, and C. L. Vernold, "Modified Beckmann-Kirchhoff scattering model for rough surfaces with large incident and scattering angles," *Opt. Eng.*, vol. 46, no. 7, 2007, Art. no. 078002.
[19] K. Haneda *et al.*, "5G 3GPP-like channel models for outdoor urban microcellular and macrocellular environments," in *Proc. IEEE 83rd Veh. Technol. Conf.*, May 2016, pp. 1–7.
[20] K. Haneda *et al.*, "Indoor 5G 3GPP-like channel models for office and shopping mall environments," in *Proc. IEEE Int. Conf. Commun. Workshops*, May 2016, pp. 694–699.
[21] S. Sun, T. A. Thomas, T. S. Rappaport, H. Nguyen, I. Z. Kovacs, and I. Rodriguez, "Path loss, shadow fading, and line-of-sight probability models for 5G urban macro-cellular scenarios," in *Proc. IEEE Globecom Workshops*, Dec. 2015, pp. 1–7.
[22] T. S. Rappaport, F. Gutierrez, E. Ben-Dor, J. N. Murdock, Y. Qiao, and J. I. Tamir, "Broadband millimeter-wave propagation measurements and models using adaptive-beam antennas for outdoor urban cellular communications," *IEEE Trans. Antennas Propag.*, vol. 61, no. 4, pp. 1850–1859, Apr. 2013.
[23] T. Abbas, J. Nuckelt, T. Krner, T. Zemen, C. F. Mecklenbruker, and F. Tufvesson, "Simulation and measurement-based vehicle-to-vehicle channel characterization: Accuracy and constraint analysis," *IEEE Trans. Antennas Propag.*, vol. 63, no. 7, pp. 3208–3218, Jul. 2015.
[24] T. Gaugel, L. Reichardt, J. Mittag, T. Zwick, and H. Hartenstein, "Accurate simulation of wireless vehicular networks based on ray tracing and physical layer simulation," in *High Performance Computing in Science and Engineering (Transactions of the High Performance Computing Center, Stuttgart)*. Berlin, Germany: Springer, 2012, pp. 619–630.
[25] C. Sommer, D. Eckhoff, R. German, and F. Dressler, "A computationally inexpensive empirical model of IEEE 802.11p radio shadowing in urban environments," in *Proc. 8th Int. Conf. Wireless On-Demand Netw. Syst. Services*, 2011, pp. 84–90.
[26] J. Nuckelt, T. Abbas, F. Tufvesson, C. Mecklenbrauker, L. Bernado, and T. Kurner, "Comparison of ray tracing and channel-sounder measurements for vehicular communications," in *Proc. IEEE 77th Veh. Technol. Conf.*, 2013, pp. 1–5.
[27] T. Yilmaz and O. B. Akan, "On the use of low terahertz band for 5G indoor mobile networks," *Comput. Elect. Eng.*, vol. 48, pp. 164–173, 2015.
[28] D. Turchinovic, A. Kammoun, P. Knobloch, T. Dobberitn, and M. Koch, "Flexible all-plastic mirrors for the THz range," *Appl. Phys. A*, vol. 74, pp. 291–293, 2002.
[29] R. Piesiewicz *et al.*, "Short-range ultra-broadband terahertz communications: Concepts and perspectives," *IEEE Antennas Propag. Mag.*, vol. 49, no. 6, pp. 24–39, Dec. 2007.
[30] N. Krumbholz *et al.*, "Omnidirectional terahertz mirrors: A key element for future terahertz communication systems," *Appl. Phys. Lett.*, vol. 88, 2006, Art. no. 202905.
[31] I. Stevanovic, A. Skrivervik, and J. R. Mosig, "Smart antenna systems for mobile communications," Tech. Rep., 2003.
[32] H. Yu-Xue, "Smart antenna technology," *Radio Commun. Technol.*, vol. 4, p. 10, 2006.

Michael Taynnan Barros was born in Campina Grande, Brazil, in 1990. He received the B.Tech. degree in telematics from the Federal Institute of Education, Science and Technology of Paraiba, Jardim Sorrilandia, Brazil, in 2011, the M.Sc. degree in computer science from the Federal University of Campina Grande, Campina Grande, in 2012, and the Ph.D. degree in telecommunication software from Waterford Institute of Technology (WIT), Waterford, Ireland, in 2016.

He is currently an IRC Government of Ireland Postdoctoral Fellow associated with the Telecommunications Software and Systems Group, WIT. He is also working with EU-funded H2020 projects, including CogNet and Circle. His research experience concentrates on vehicular ad hoc networks, cognitive network management, molecular communication, and terahertz communication. He has authored or coauthored more than 35 papers in international journals and conferences. He is also a reviewer for many journals and participated as technical program committee and reviewer for various international conferences. His research interests include nanonetworks, molecular communication, terahertz communication, and 5G for both connected-health and connected-cars.

Robert Mullins received the B.S. degree in computer science and mathematics and M.S. degree in computer science from University College Cork, Cork, Ireland, in 1990 and 1993, respectively.

Since joining Telecommunication Software and Systems Group, Waterford Institute of Technology, Waterford, Ireland, in 2005, he has managed the IMS ARCS Academic Consortium, which focused on providing research and development in IP multimedia system technology, together with business and marketing analysis to a consortium of Irish companies involved in the telecommunications industry. He also has a long track record in European Research having participated in various roles in FP6 and FP7 projects including ICT Daidalos. His one of the most recent activities involved leading an EU-commission-sponsored group developing a roadmap for future research in the application of artificial intelligence methods to software engineering problems, particularly in the area of the automatic adaptation and evolution of software systems and of improving and automating the software development and maintenance processes. Most recently, he has successfully coordinated the H2020 5GPPP CogNet proposal. This project is focused on next-generation autonomic network management systems and the application of machine learning algorithms to manage quality of service and quality of experience for 5G networks and the Internet of Things.

Sasitharan Balasubramaniam (SM'14) received the B.S. degree in electrical and electronic engineering from the University of Queensland, Brisbane, Australia, in 1998, the M.S. degree in computer and communication engineering from Queensland University of Technology, Brisbane, in 1999, and the Ph.D. degree in computer science from the University of Queensland in 2005.

He is a Senior Research Fellow with the Nano Communication Centre, Department of Electronic and Communication Engineering, Tampere University of Technology, Tampere, Finland. He was a Research Fellow with the Telecommunication Software and Systems Group, Waterford Institute of Technology, Waterford, Ireland, where he worked on a number of Science Foundation Ireland projects. He has authored or coauthored more than 70 papers and actively participated in a number of technical program committees for various conferences. His current research interests include bioinspired communication networks and molecular communications.

Dr. Balasubramaniam was the co-Founder and TPC co-Chair for the 2014 ACM International Conference on Nanoscale Computing and Communication and the 2011 IEEE International Workshop on Molecular and Nano Scale Communication. He is an Editor for the IEEE INTERNET OF THINGS and *Nano Communication Networks*.